HHS Public Access

Author manuscript

J Immunol. Author manuscript; available in PMC 2023 December 15.

Published in final edited form as:

J Immunol. 2023 June 15; 210(12): 1913–1924. doi:10.4049/jimmunol.2200871.

Severe CD8+ T lymphopenia in WHIM syndrome caused by selective sequestration in primary immune organs

Shamik Majumdar[*], **Sergio M. Pontejo**[*], **Hemant Jaiswal**[*], **Ji-Liang Gao**[*], **Abigail Salancy**[*], **Elizabeth Stassenko**[†], **Hidehiro Yamane**[†], **David H. McDermott**[*], **Karl Balabanian**[‡], **Françoise Bachelerie**[§], **Philip M. Murphy, M. D.**[*,¶]

[*]Laboratory of Molecular Immunology, National Institute of Allergy and Infectious Diseases, National Institutes of Health, Bethesda, Maryland, United States

[†]Laboratory of Cellular and Molecular Biology, Center for Cancer Research, National Cancer Institute, National Institutes of Health, Bethesda, Maryland, United States

[‡]Université Paris-Cité, Institut de Recherche Saint-Louis, OPALE Carnot Institute, EMiLy, INSERM U1160, Paris, France.

[§]Université Paris-Saclay, INSERM, Inflammation, Microbiome and Immunosurveillance, Orsay, France.

Abstract

WHIM (warts, hypogammaglobulinemia, infections and myelokathexis) syndrome is an ultra-rare combined primary immunodeficiency disease caused by heterozygous gain-of-function mutations in the chemokine receptor CXCR4. WHIM patients typically present with recurrent acute infections associated with myelokathexis (severe neutropenia due to bone marrow retention of mature neutrophils). Severe lymphopenia is also common but the only associated chronic opportunistic pathogen is HPV and mechanisms are not clearly defined. Here we show that WHIM mutations cause more severe CD8 than CD4 lymphopenia in WHIM patients and WHIM model mice. Mechanistic studies in mice revealed selective and WHIM allele dose-dependent accumulation of mature CD8 single positive (SP) cells in thymus in a cell-intrinsic manner due to prolonged intrathymic residence, associated with increased CD8 SP thymocyte chemotactic responses *in vitro* towards the CXCR4 ligand CXCL12. In addition, mature WHIM $CD8^+$ T cells preferentially home to and are retained in the bone marrow in mice in a cell-intrinsic manner. Administration of the specific CXCR4 antagonist AMD3100 (plerixafor) in mice rapidly and transiently corrected T cell lymphopenia and the CD4/CD8 ratio. After LCMV infection, we found no difference in memory $CD8^+$ T cell differentiation or viral load between wild type and WHIM model mice. Thus, lymphopenia in WHIM syndrome may involve severe CXCR4-dependent

[¶]**Corresponding author:** Philip M. Murphy, M. D., Bldg. 10, Room 11N111, NIH, Bethesda, MD 20892; Tel: 301-496-8616; Fax: 301-402-4369; pmm@nih.gov.

Author contributions

The experimental design was provided by SM, SMP, HJ, JLG and PMM. Generation and experimental data were provided by SM, SMP, HJ, ES, HY and AS with supervision and analysis by JLG, DM and PMM. KB and FB provided the WHIM mouse model. The manuscript was written mainly by SM and PMM with contributions from all authors.

Disclosure of Conflicts of Interest

All authors have declared that no conflict of interest exists.

$CD8^+$ T cell deficiency resulting in part from sequestration in the primary lymphoid organs, thymus and bone marrow.

Keywords

AMD3100 (plerixafor); bone marrow; CD4/CD8 ratio; cell migration; CXCL12; LCMV; thymus

Introduction

CXCR4 is constitutively expressed in most tissues and leukocyte subsets, and regulates organogenesis, hematopoiesis and leukocyte trafficking (1–4). Mutations in the CXCR4 *C*-terminal domain cause the ultra-rare, autosomal dominant, primary immunodeficiency disorder WHIM syndrome (OMIM # 193670).

WHIM mutations eliminate phosphorylation sites required for β-arrestin recruitment and CXCR4 internalization, thereby blunting receptor downregulation and enhancing CXCR4 signaling (5, 6). This amplifies CXCR4 signals that normally restrain neutrophil egress from bone marrow (BM) and promote homing of senescent neutrophils to BM (7). The net result is myelokathexis, which is characterized by myeloid hyperplasia, neutropenia, and dysmorphic apoptotic BM neutrophils. B cell lymphopenia is also common and is associated with moderate hypogammaglobulinemia. Neutropenia and hypogammaglobulinemia are thought to drive recurrent acute infection with common bacterial pathogens in WHIM patients (8).

Susceptibility to HPV is less well understood, but may involve T cell-dependent immunodeficiency. In this regard, circulating $CD4^+$ and $CD8^+$ T cells are reduced in most WHIM patients (8–10). Furthermore, reports of skewed TCR diversity and reduced levels of recent thymic emigrants (RTEs) (9, 11, 12) suggest a thymic defect. Although mice completely lacking *Cxcr4* or its ligand *Cxcl12* are non-viable (2, 4), knockout embryos and conditionally *Cxcr4*-deficient mice have indicated that Cxcr4 promotes thymic homing of T cell progenitors (13–15) as well as T cell survival and proliferation at early stages of development (16, 17). However, mice deficient in Cxcr4 from the double positive (DP) stage onwards show normal cellularity at the DP stage onwards and normal splenic T cell numbers and distribution, suggesting that CXCR4 signaling is dispensable for αβ T cell development (18). Despite these insights, the mechanisms underlying T lymphopenia and the role of CXCR4 signaling during T cell development in WHIM syndrome are not fully defined (10). Here, we addressed this gap by studying T cell development and distribution in CXCR4 S338X WHIM model mice (19).

Methods

Patients

WHIM patients were recruited to a clinical research protocol approved by the Institutional Review Board of the National Institutes of Health consistent with the Declaration of Helsinki. The diagnosis of WHIM patients was established by the presence of compatible clinical manifestations, including at a minimum severe sustained neutropenia (absolute

neutrophil count < 500 cells/microliter of whole blood) and a damaging heterozygous mutation located in the region of the *CXCR4* open reading frame that encodes the *C*-terminal domain of the receptor. All subjects gave informed written consent.

Mice

Five-eight-week old mice of either sex were used. Development of $Cxcr4^{+/1013}$(+/*w*) WHIM mice on a C57BL/6 background has been described (19). The nucleotide change at position 1013 is the second-most common WHIM mutation and introduces a stop codon for codon Ser338. Congenic wild type $Cxcr4^{+/+}$ (+/+), heterozygous $Cxcr4^{+/1013}$ (+/*w*) or homozygous $Cxcr4^{1013/1013}$ (*w*/*w*) mice were obtained by breeding either +/+ and +/*w* mice or +/*w* and +/*w* mice. For transplantation studies, the +/+ and +/*w* mice were crossed with C57BL/6 mice polymorphic for CD45.1 or CD45.2 to mark cells from competing donor and recipient cells (20). Recombination-activating gene-green fluorescent protein (RAG-GFP) mice have been described (21). All mice were maintained in a specific pathogen-free NIH facility under a 12 h light/dark cycle and had access to water and food *ad libitum*. The study was reviewed and approved by the Animal Care and Use Committee of NIAID.

Cell enumeration

Cell suspensions were diluted in PBS (Thermo Fisher Scientific, Waltham, MA, U.S.A) prior to mixing in a ratio of 1:1 with ViaStain™ AOPI Staining Solution (Nexcelom Bioscience, Lawrence, MA, U.S.A). The cell numbers were counted using the Cellometer Auto 2000 Cell Viability Counter (Nexcelom Bioscience). By flow cytometry, the frequencies and absolute numbers of cell subsets were calculated.

Tissue processing and cell enumeration

Maxillary vein blood was collected in EDTA-coated tubes (Sarstedt, Nümbrecht, Germany). The harvested organs were pressed through 0.7 μm cell strainers. Erythrocytes were lysed using ACK lysis buffer (Quality Biological™, Gaithersburg, MD, U.S.A). BM was flushed and resuspended with RPMI-1640 (Thermo Fisher Scientific) containing 10% FBS (GeminiBio™, West Sacramento, CA, U.S.A) and 2 mM EDTA (MilliporeSigma, Burlington, MA, U.S.A).

For LCMV challenge experiments, spleens were collected on day 8 post-infection, and splenocytes were dissociated with Liberase™ (0.25 mg/mL, MilliporeSigma) at 37°C for 15 mins, then passed through 0.7 μm cell strainers followed by erythrocyte lysis. Cells were washed and resuspended in lymphocyte medium (RPMI-1640 containing 10% FBS, Penicillin-Streptomycin, HEPES, 2-Mercaptoethanol, MEM Non-Essential Amino Acids Solution and Sodium Pyruvate, Thermo Fisher Scientific).

Flow cytometry

The peripheral blood mononuclear cells (PBMCs) from healthy donors (HDs) and WHIM syndrome patients were stained for FACS at 4°C for cell-surface expression of CD45, CD3, CD4 and CD8. Subsequently, the cells were washed with PBS, and fixed with 1.0% formaldehyde prior to resuspension in PBS. The samples were acquired on a BD FACSLyric™ (BD Biosciences, Franklin Lakes, NJ, U.S.A) and the results were analyzed

using FCS Express 6 Flow Cytometry Clinical Edition (22) (De Novo™ Software, Pasadena, CA, U.S.A).

For mice, blood samples or single cell suspensions of splenocytes, thymocytes, BM cells or LNs were incubated with the viability dyes Zombie UV™ (BioLegend®, San Diego, CA, U.S.A) or LIVE/DEAD™ Aqua (Thermo Fisher Scientific), according to the manufacturer's instructions. Next, the Fc receptors were blocked using anti-CD16/CD32 monoclonal antibodies for 10 mins at 4°C. The fluorescently-labeled monoclonal antibodies specific to cell-surface markers were added to the samples, and were stained for 45 mins in the dark at 4°C. Prior to acquisition on the flow cytometer, the samples were washed with FACS buffer (PBS containing 2% FBS and 2 mM EDTA) and were resuspended in the same. All flow cytometry analyses were performed on single, live events. The antibodies used for FACS analysis are listed in Table S1 and gating strategy for thymocyte analysis is provided in Fig. S1. Briefly, the DN, DP and SP thymocyte subsets were gated on the basis of CD4 and CD8 expression. For quantification of SP subsets, CD4 SP and CD8 SP cells were gated and plotted on CD24 versus TCRβ plots, and the $CD24^{high(hi)}TCR\beta^{+}$ and $CD24^{low(lo)}TCR\beta^{+}$ cells were gated and quantified (23–25). For quantification of mouse T cells in blood, spleen and the lymph nodes, the cells were analyzed by initially gating on CD45-isoform expression. The $CD4^{+}$ and $CD8^{+}$ T cells in the $CD45^{+}$ gate were quantified.

For quantification of LCMV-specific T cells, splenocytes were stained with LIVE/DEAD™ Aqua along with Fc blocking solution and antibodies against CD127, KLRG1, CD8 and GP33-MHC-I tetramers (NIAID tetramer core facility, Emory Vaccine Center, Emory University, Atlanta, GA) at 4°C for 30 mins. To stain for intracellular cytokines, the splenocytes were stimulated with GP33 peptide (200 pg/mL, Peptide 2.0 Inc, Chantilly, VA, U.S.A) for 4 h with protein transport inhibitor cocktail (Thermo Fisher Scientific). Subsequently, the cells were stained with LIVE/DEAD™ Aqua and antibodies against CD44 and CD8. After cell surface staining, fixing and permeabilization, the intracellular molecules were stained. The cells were resuspended in PBS prior to acquiring data on the flow cytometer (26).

Transplantation experiments

BM was harvested from +/+ (CD45.1/.2) and +/*w* (CD45.2) mice expressing RAG-GFP. The T cells were depleted using the CD3ε MicroBead kit (Miltenyi Biotec, Bergisch Gladbach, North Rhine-Westphalia, Germany) and the autoMACS® Pro Separator (Miltenyi Biotec). T cell-depleted +/+ and +/*w* BM cell suspensions were mixed 1:1, and ~5×10^{6} cells per mouse were injected via tail vein in sex-matched +/+ and +/*w* recipient/host mice 6–8 h after lethal irradiation (9 Gy). The irradiated mice were provided with neomycin-supplemented water for 4 weeks (20). After 8–10 weeks of BM reconstitution, recipient organs were analyzed (27).

Homing assays

Cell suspensions from spleen, mesenteric lymph node (mLN) and inguinal lymph nodes (iLNs) from naïve +/+ or +/*w* mice expressing either CD45.1 or CD45.2 were obtained, and mixed 1:1 and resuspended in RPMI-1640 containing 1X Penicillin-Streptomycin. 15–

20×10^6 cells per mouse were i.v-injected into CD45.1/.2 +/+ and +/*w* mice. After 24 h, T cell composition was analyzed in recipient mouse organs. The homing index of +/*w* T cells was calculated as the output ratio of +/*w* T cells versus +/+ T cells, divided by the input ratio of +/*w* T cells versus +/+ T cells. The input ratio varied slightly between experiments but the above index corrected for differences in composition between T cells of +/+ and +/*w* mice (28).

Chemotaxis assays

For each experiment, thymocytes were pooled from 4 +/+ or 4 +/*w* mice, divided in two and each part was enriched for CD4 or CD8 SPs by negative selection using $CD4^+$ T cell and $CD8a^+$ T cell isolation kits and magnetic-activated cell sorting following the manufacturer's recommendation (Miltenyi Biotec). The 4 SP subsets were labeled differently (x1 unstained, x1 double stained, x2 single stained) using green and violet calcein AM (BioLegend®). Of note, different calcein labeling patterns were used in different experiments to rule out possible artifacts introduced in our cell migration assays caused by the distinct calcein staining of each SP subset. Then, equal total numbers of the 4 calcein-labeled SP subsets were pooled together and resuspended in assay buffer (RPMI-1640 supplemented with 10 mM HEPES and 0.5% BSA, MilliporeSigma) at 8×10^6 total cells/mL. Where indicated, increasing concentrations of recombinant mouse CXCL12 (PeproTech, Rocky Hill, NJ, U.S.A) were added in quadruplicate to the bottom wells of a 96-well ChemoTx transwell plate (Neuro Probe, Gaithersburg, MD, U.S.A) and 2×10^5 cells/well (50,000 cells from each SP subset) were placed on top of a 5 μm pore-sized membrane. Cells were allowed to migrate for 90 mins at 37°C, and cells migrated to the bottom well were counted and analyzed by FACS. For each SP subset, the chemotaxis index was calculated as the ratio of migrated cells at a given CXCL12 concentration over spontaneous migration to buffer alone.

AMD3100 treatment

Mice received 10 mg/kg of plerixafor (Sanofi, Paris) in 0.2 mL PBS i.p. At 2.5 h post-injection, blood leukocytes were quantitated by FACS, as described (29).

LCMV infections and serum virus load estimation

Mice were injected i.p. with 2×10^5 plaque-forming units of LCMV. On days 4 and 8 post-infection, blood was collected for viral RNA estimation. Quantification of LCMV-specific T cells and *in vitro* peptide stimulation for intracellular cytokine measurement were performed as described (26). On days 4 and 8 post infection, serum samples from peripheral blood were collected. Viral RNA was extracted using the PureLink Viral RNA/DNA mini kit (Invitrogen, Thermo Fisher Scientific) according to the manufacturer's instructions. Next, the isolated RNA was reverse transcribed using QuantiTect reverse transcription kit (Qiagen, Hilden, Germany). By real-time PCR with the PowerUp™ SYBR™ Green master mix, the cDNA was quantified (Applied Biosystems; Thermo Fisher Scientific) on a QuantStudio 3 real time system (Applied Biosystems). The primers used to quantify the transcripts specific for the LCMV segment S envelope glycoprotein (GP) gene were (Forward-CATTCACCTGGACTTTGTCAGACTC, Reverse-GCAACTGCTGTGTTCCCGAAAC) (26).

Statistical analysis

Differences were analyzed using GraphPad Prism (GraphPad Software, La Jolla, CA, U.S.A). For one-way ANOVA analyses, data sets were checked for heteroscedasticity using the Brown-Forsythe and Bartlett's test. Tukey's or Dunnett's multiple comparisons test were used for data sets with equal or significantly different SD, respectively. The data are presented as mean ± SEM or mean ± SD, as indicated in the figure legends.

Study approval

All mouse experiments were performed using an NIAID Animal Care and Use Committee-approved protocol in approved and certified facilities.

Results

Elevated blood CD4/CD8 ratio in WHIM patients and WHIM model mice

We first determined circulating $CD4^+$ and $CD8^+$ T cell counts for 30 WHIM patients who showed no signs of active infection and were not receiving G-CSF or immunoglobulin supplementation. Approximately 75% were at or well-below the lower limit of normal, independent of age (Fig. 1A and 1B). The mean CD4/CD8 ratio was elevated by ~3-fold compared with healthy donors (n=39), revealing a disproportionate deficiency of $CD8^+$ T cells over $CD4^+$ T cells (Fig. 1C).

Similarly, in mice the circulating $CD8^+$ T cell frequency within the $CD3^+$ gate declined in a CXCR4 S338X WHIM allele dose-dependent manner; consequently, the proportions of $CD4^+$ T cells were increased (Fig. 1D, left panel). The absolute numbers of both circulating $CD4^+$ and $CD8^+$ T cells were reduced in *+/w* mice and further reduced in *w/w* mice (Fig. 1D, right panel). Circulating CD4/CD8 ratios were elevated in a WHIM allele dose-dependent manner (Fig. 1E). Therefore, the WHIM *CXCR4* mutation in both mice and humans depressed circulating $CD8^+$ T cell counts more severely than $CD4^+$ T cell counts.

WHIM thymi accumulate mature CD8 single positive cells

To test the contribution of the thymus to T lymphopenia in WHIM syndrome, we investigated T cell development in 5–8 week old *+/+, +/w* and *w/w* littermates. The thymi of S338X WHIM mice are reported to have ~30% reduced cellularity than their *+/+* counterparts, resulting in all the major thymocyte subsets namely, DN, DP, CD4 and CD8 SP thymocytes, being significantly reduced (19, 30). While we did observe that the total thymic cellularity trended lower in the presence of the WHIM allele, the number of thymocytes obtained from *+/+* and *+/w* mice did not vary significantly (Fig. S2A). We found a small decrease in DP cell frequency in *w/w* mice, whereas the proportion of SP cells increased (Fig. S2B, C). Similarly, while the total DP cell number was reduced in *w/w* mice, thymic CD4 and CD8 SP cell content increased. However, only CD8 SP numbers increased in a clear WHIM allele dose-dependent manner (Fig. 2A). Conversely to the blood, the intrathymic CD4/CD8 ratio declined in a WHIM allele dose-dependent manner (Fig. 2B), indicating disproportionately more CD8 SP thymocytes than CD4 SPs in WHIM mouse thymi.

We next analyzed expression of the maturation markers CD24 (heat-stable antigen) and TCRβ on SP cells. Semi-mature SP cells are $CD24^{hi}TCR\beta^{+}$ whereas mature SP cells are $CD24^{lo}TCR\beta^{+}$ (23–25). Compared to +/+ littermate controls, *w*/*w* but not +/*w* mice displayed a small increase in mature $CD24^{lo}TCR\beta^{hi}$ CD4 SP cells (Fig. 2C, D). Consistent with this, CD4 SP $CD24^{hi}/CD24^{lo}$ cell ratios were reduced only in *w*/*w* mice when compared to +/+ mice (Fig. 2D). In contrast, in the CD8 SP compartment there was a marked WHIM allele dose-dependent increase in absolute number of mature $CD24^{lo}TCR\beta^{hi}$ cells (Fig. 2F and 2G), whereas the absolute numbers of semi-mature $CD24^{hi}TCR\beta^{hi}$ CD8 SP cells were similar in all three groups (Fig. 2G). Consequently, CD8 SP $CD24^{hi}/CD24^{lo}$ ratios decreased in a WHIM allele dose-dependent manner (Fig. 2H). Thus, peripheral $CD8^{+}$ T cell lymphopenia in WHIM mice is not due to defective thymic development. Moreover, the increase in intrathymic CD8 SP cells was accounted for by increased mature CD8 SP cells.

Accumulation of intrathymic WHIM CD8 single positive thymocytes is cell-intrinsic and occurs due to prolonged thymic residence

Since all WHIM syndrome patients are heterozygous and not homozygous for the CXCR4 gain-of-function mutation, we restricted the remainder of the experiments in this study to +/+ and +/*w* mice. To address mechanisms of intrathymic accumulation of CD8 SPs in WHIM mice, we performed competitive transplantation experiments in lethally irradiated +/+ and +/*w* recipient mice reconstituted with BM from +/+ and +/*w* mice expressing RAG-GFP, which allows quantitation of the relative duration of thymic residence (27) and identification of RTEs, and distinguishes recirculating T cells from thymocytes (21, 31, 32). Importantly, we previously reported that baseline frequencies of HSCs in BM from WT and WHIM mice are similar (33). Donor +/+ and +/*w* thymocytes comprised ~78% and 20%, respectively, of total thymocytes 8–10 weeks after reconstitution, regardless of host genotype. This difference aligns with the reported engraftment disadvantage of +/*w* BM compared to +/+ and +/o BM in competitive transplantation experiments in mice (33).

CD8 SP frequencies were increased for donor +/*w* thymocytes compared with donor +/+ thymocytes in both +/+ and +/*w* recipients, whereas frequencies were similar for double negative (DN), DP and CD4 SP cells (Fig. 3A–D). The CD4/CD8 SP ratio was decreased for donor +/*w* thymocytes (Fig. 3E). Furthermore, the donor +/+:+/*w* frequency ratio was below 1 for CD8 SP cells, but not for CD4 SP cells, in both recipient groups (Fig. 3F), which indicates that the WHIM mutation promotes intrathymic accumulation of CD8 but not CD4 SPs.

Consistent with results in naïve mice, the frequencies of $CD24^{hi}$CD8 SP and $CD24^{lo}$CD8 SP thymocytes among total CD8 SP were decreased and increased, respectively, for the +/*w* donor compared with the +/+ donor in both recipient groups (Fig. 3G, H). Increased CD8 SP content in the thymus could result from WHIM allele-dependent effects on thymic residence time (27) and/or $CD8^{+}$ T cell recirculation in the thymus (31, 32), which we measured by RAG-GFP expression. $RAG\text{-}GFP^{+}$ cell frequencies in the $TCR\beta^{+}$ SP compartments were similar for +/+ and +/*w* donors in both +/+ and +/*w* recipients, and all frequencies exceeded 90%, indicating that recirculating T cells ($RAG\text{-}GFP^{-}$) did not contribute significantly to the

increased intrathymic WHIM CD24^{lo}CD8 SP frequencies (Fig. 3I). In addition, while donor +/+ and +/*w* TCRβ^{+}CD4 SPs expressed similar levels of RAG-GFP (+/+:+/*w* RAG-GFP MFI ratio = 1), donor +/*w* TCRβ^{+}CD8 SPs expressed lower RAG-GFP levels than donor +/+ TCRβ^{+}CD8 SPs (+/+:+/*w* RAG-GFP MFI ratio > 1) in both recipient groups (Fig. 3J). These results indicate that the accumulation of mature WHIM CD8 SPs is cell-intrinsic and that the WHIM mutation prolongs the thymic residence time of these cells.

WHIM CD8 single positive cells show heightened CXCL12-induced chemotaxis

CXCR4 downregulation during T cell development is crucial for SP intrathymic trafficking (27). Therefore, we next studied cell-surface CXCR4 levels and chemotactic responses of thymocytes from naïve +/+ and +/*w* mice. In agreement with the literature (18), CXCR4 expression was high on DN and DP thymocytes and downregulated in SPs, with CD8 SPs expressing higher CXCR4 surface levels than CD4 SPs (Fig. 4A), indicating that CXCR4 regulation was normal on WHIM thymocytes. Since our previous data pointed to CD8 SP as the major thymic population affected by the *Cxcr4*^{1013} WHIM mutation, we compared CXCL12 chemotactic responses of +/+ and +/*w* SP thymocytes. The overall migration of the SP pool peaked at 1 nM of CXCL12 and aligned with the expected bell-shaped dose-response curve (Fig. 4B). +/*w* CD8 SPs displayed a markedly higher response than any other SP subset (Fig. 4C). The relative rank order of migration was +/*w* CD8 SP > +/+ CD8 SP > +/*w* CD4 SP ≥ +/+ CD4 SP. Higher chemotactic responsiveness by +/*w* CD8 SP might delay their migration from the CXCL12-rich cortex to the medulla and explain prolonged thymic residence time and intrathymic accumulation. In addition to CXCR4, we also quantified cell-surface expression of CCR7, CCR9 and S1PR1, molecules that critically influence thymocyte development, migration and egress (34). CCR7 and CCR9 levels on WHIM TCRβ^{+} SPs were observed to be normal compared to WT TCRβ^{+} SPs (Fig. S2D, E). The expression of S1PR1 on mature (TCRβ^{+}CD69^{lo}MHC-I^{hi}) WT and WHIM SPs was also comparable (Fig. S2F).

Cxcr4 WHIM mutation promotes accumulation of CD8 T cells in the bone marrow

We next quantified T cells in the BM, spleen and mLN of +/+ and +/*w* mice. +/*w* BM had higher CD4^{+} and CD8^{+} T cell content than +/+ mouse BM, with more CD8^{+} than CD4^{+} T cells (Fig. 5A). However, increased T cell content was not observed in mLN of +/*w* mice. Similar to the blood (Fig. 1), +/*w* mice presented lower CD4^{+} and CD8^{+} T cell numbers in the spleen (Fig. 5A). In addition, unlike +/*w* BM, both +/*w* spleen and +/*w* mLN contained fewer CD8^{+} than CD4^{+} T cells (Fig. 5A).

To understand why CD8^{+} T cell content is elevated in +/*w* BM, we performed homing experiments (Fig. 5B) as previously described (28). +/*w* CD4^{+} and CD8^{+} T cells had greater BM homing capacity than +/+ T cells (homing index > 1) in both recipient mouse groups (Fig. 5C). However, donor +/*w* cells had no advantage (homing index ≤ 1) in homing to the mLN, while +/*w* CD8^{+} T cells demonstrated a small but significant homing advantage to the +/*w* spleen (Fig. 5C). Interestingly, +/*w* CD8^{+} T cells showed higher BM homing capacity than +/*w* CD4^{+} T cells in +/*w* but not +/+ host mice (Fig. 5C).

To address whether increased BM T cell content in +/*w* mice was cell-intrinsic, we transplanted +/+ and +/*w* mice with BM cells from +/+ and +/*w* mice expressing RAG-GFP. The +/+ and +/*w* donor BM-derived $CD45^+$ cells comprised an average of 76% and 24% of total $CD45^+$ cells in the reconstituted host BM, respectively. While the distributions of donor $CD4^+$ T cells were similar, the frequency of +/*w* donor $CD8^+$ T cells exceeded that of +/+ donor $CD8^+$ T cells in cotransplanted +/+ recipients, but not in +/*w* hosts (Fig. 5D, E). However, the CD4/CD8 ratio of +/*w* donor cells was markedly lower than that of +/+ transplanted cells in both recipient groups (Fig. 5F), indicating that the WHIM mutation promotes greater accumulation of $CD8^+$ than $CD4^+$ T cells in the BM. Importantly, disproportionate accumulation of +/*w* donor $CD8^+$ T cells was not observed in any other analyzed tissue (Fig. S3). Therefore, WHIM $CD8^+$ T cells preferentially home to and are retained in the BM in a cell-intrinsic manner.

WHIM syndrome patients have been reported to possess low numbers of circulating RTEs (9, 11). Therefore, we investigated RTE frequencies (RAG-GFP^+ T cells) in the BM of reconstituted mice. For $CD4^+$ T cells, the frequencies of +/*w* $CD4^+$ RTEs exceeded those of +/+ $CD4^+$ RTEs in both recipient groups (Fig. 5G), whereas the pattern of $CD8^+$ RTE frequency was both donor- and recipient-dependent (Fig. 5H). Consequently, differences in CD4/CD8 RTE ratios between +/+ and +/*w* donor T cells were also host-dependent (Fig. 5I). We concluded that with the exception of donor $CD8^+$ RTEs in +/+ host mice, the frequency of both +/*w* $CD4^+$ and $CD8^+$ RTEs was elevated in the BM, possibly contributing towards sequestering RTEs from the circulation.

Cxcr4 WHIM mutation does not affect $CD8^+$ T anti-LCMV responses

To address the impact of the WHIM mutation on anti-viral $CD8^+$ T cell-dependent immune responses, we analyzed mice acutely infected with the Armstrong strain of LCMV (35). We found that overall cellularity and absolute numbers of $CD8^+$ T cells in the spleens of +/*w* mice were lower than in +/+ mice both before and after infection, but an increase of $CD8^+$ T cell counts was observed upon LCMV infection (Fig. 6A, B). The LCMV burden in the sera was similar in +/+ and +/*w* mice on day 4 post infection, whereas on day 8 viral burden was higher in +/*w* than +/+ mice, possibly due to low $CD8^+$ T cell numbers in +/*w* mice (Fig. 6C). Nonetheless, the proportions of LCMV-specific $CD8^+$ T cells for the immunodominant LCMV epitope GP33 were similar in +/+ and +/*w* mice (Fig. 6D). Upon infection, virus-specific $CD8^+$ T cells differentiate into memory precursor effector cells (MPECs, $KLRG1^{lo}CD127^{hi}$) or short-lived effector cells (SLECs, $KLRG1^{hi}CD127^{lo}$) (26). It has been reported that CXCR4 overexpression in activated $CD8^+$ T cells is associated with a higher frequency of MPECs and lower frequency of SLECs (36). MPEC and SLEC frequencies were comparable among GP33-specific $CD8^+$ T cells of infected +/+ and +/*w* mice (Fig. 6E). Furthermore, the frequencies of $GP33^+$ +/+ and +/*w* $CD8^+$ T cells expressing the cytotoxic molecule granzyme B after LCMV infection *in vivo* (Fig. 6F), and the frequency of $CD44^+CD8^+$ cells from LCMV-infected +/+ and +/*w* mice producing IFN-γ, IFN-γ+TNF-α or IFN-γ+IL-2 after *ex vivo* stimulation with the GP33 peptide were largely comparable (Fig. 6G). Thus, expansion and differentiation of competent anti-viral antigen-specific $CD8^+$ T cells are intact in WHIM mice in this model.

The CXCR4 inhibitor AMD3100 corrects T cell lymphopenia in WHIM mice

The CXCR4 antagonist AMD3100 (plerixafor) approved by the FDA for autologous transplantation in patients with Non-Hodgkin's Lymphoma or multiple myeloma (37) ameliorates panleukopenia in both WHIM patients (8, 38–40) and WHIM mice (19). However, previous studies in the mouse model did not specifically address the effect of AMD3100 on $CD4^+$ and $CD8^+$ T cells. AMD3100-induced leukocyte release is known to peak in mice at ~2.5 h after subcutaneous injection (29). Therefore, to investigate whether CXCR4 inhibition could correct CD8 lymphopenia in WHIM mice, we studied blood leukocytes in +/+ and +/*w* mice ~2.5 h after administering a bolus 10 mg/kg i.p. dose of AMD3100. Confirming previously published results (19, 29), we observed a large surge of leukocytes in +/+ and +/*w* mice upon AMD3100 treatment that equalized the total leukocyte counts in the blood between these mouse groups (Fig. 7A). Furthermore, AMD3100 treatment successfully corrected $CD4^+$ and $CD8^+$ T lymphopenia (Fig. 7B), and restored the CD4/CD8 T cell blood ratio to normal in +/*w* mice (Fig. 7C).

Discussion

In this study, we provide evidence that T cell lymphopenia in WHIM syndrome is driven asymmetrically by severe $CD8^+$ T cell lymphopenia in both WHIM patients and WHIM model mice, which may be caused at least in part by sequestration of $CD8^+$ T cells in the two primary lymphoid organs, thymus and BM, but not in secondary lymphoid organs, LN and spleen (Table 1). This might be explained by multiple factors including constitutive production of CXCL12 by the thymic cortex (14, 18) and BM endothelium (28, 41), CXCR4- and CXCL12-dependent and -independent homing of $CD8^+$ T cells in the BM and spleen, respectively (28, 42, 43), and higher CXCR4 expression by BM $CD8^+$ compared to BM $CD4^+$ T cells or splenic T cells (28, 44). Moreover, we show that severe $CD8^+$ T lymphopenia in WHIM mice does not preclude a normal virus-specific $CD8^+$ T cell immune response, which aligns with the paucity of opportunistic viral infections apart from HPV in patients with WHIM syndrome. Our results also support the clinical usage of AMD3100 to maintain normal $CD4^+$ and $CD8^+$ T cell counts in the blood of WHIM syndrome patients. To our knowledge, this is the first report using a human genetic disease model that connects prolonged thymic residence of mature CD8 SPs with peripheral $CD8^+$ T cell cytopenia.

We found that sequestration of $CD8^+$ SP thymocytes in the thymus affected mainly mature $CD24^{lo}$CD8 SP cells and involved their prolonged residence time in the thymus. The sequestration of WHIM CD8 SP cell content in the thymus was cell-intrinsic and occurred despite overall reduced cellularity in WHIM thymi. The WHIM mutation may subvert the normal process by which TCR-mediated CXCR4 downregulation allows positively selected SP thymocytes to migrate from the CXCL12-rich thymic cortex into the medulla (27, 45). In this regard, WHIM CD8 SP thymocytes displayed enhanced chemotactic responses to CXCL12 compared with WT CD8 SPs or either WT or WHIM CD4 SPs. This may be explained by the lower levels of cell-surface CXCR4 protein we detected on CD4 SPs compared to CD8 SPs, consistent with previous analysis at the transcriptional level (46). Thus, we propose that the relatively high expression levels of a hyperfunctional CXCR4 variant on CD8 SPs delays the movement of these cells from the cortex to the medulla,

resulting in prolonged thymic residence and accumulation in the thymus. Intrathymic accumulation of mature $CD24^{lo}$ CD8 SP cells in WHIM mice likely adversely affects the thymic output. However, quantification of thymic output in blood of WHIM mice would be confounded by at least two factors: reduction of T cells in blood of WHIM mice (Fig. 1D) and accumulation of WHIM RTEs in the BM of mice (Fig. 5 G–I). Our results appear to argue against the postulated notion that high levels of CXCL12 promote thymic egress by repelling CD4 SP cells in a CXCR4-dependent fugetactic manner (47, 48). Instead, and consistent with our data, it has been shown that persistent expression of CXCR4 in mice impairs the migration of TCR^{hi} thymocytes from the cortex to the medulla of the thymus, prolonging their thymic residence and increasing intrathymic SP proportions (27). Zehentmeier *et al.* recently reported that an independent line of WHIM mice carrying the most common WHIM mutation CXCR4 R334X were also lymphopenic, but, in contrast to our results, they found that the WHIM SP thymocytes did not accumulate in the thymi of naïve mice (49). Although it is unlikely that the R334X and S338X mutations have different effects on thymocyte distribution, this possibility will need to be addressed in future direct comparisons of the two lines of mice.

$CD8^+$ WHIM T cells homed more avidly from blood to BM but not mLN compared to wild type control cells, and could be readily mobilized to the blood by blocking CXCR4 with the specific antagonist AMD3100, suggesting that BM sequestration is caused by both increased homing to and increased retention in BM, both dependent on CXCR4 gain-of-function. Our results are consistent with previous reports that in mice the CXCL12/CXCR4 signaling axis is crucial for normal homing of naïve and memory $CD8^+$ T cells in the BM under homeostatic conditions (28, 42), as it is for HSCs (41) and neutrophils (7). Our results are also consistent with the recently published study on the CXCR4 R334X WHIM mouse model, wherein the authors observed high T cell content in the BM of WHIM mice due to their enhanced BM homing capacity (49). In addition, the authors of the study demonstrated that IL-7 downregulation in mesenchymal stem cells contributes towards peripheral lymphopenia in the CXCR4 R334X WHIM mice (49). While, we did not measure BM IL-7 amounts in our mice, the IL-7R (CD127) expression on WT and WHIM BM T cells was similar, along with the *ex vivo* IL-7 responsiveness with respect to phospho-STAT5 levels (Fig. S2G, H). Therefore, as in the thymus, we propose that the heightened CXCL12 responsiveness of WHIM CXCR4 promotes infiltration and accumulation of $CD8^+$ T cells into the CXCL12-rich BM, contributing to peripheral $CD8^+$ T cytopenia, which could be rapidly and transiently corrected by administration of the CXCR4 inhibitor AMD3100. We have previously demonstrated that the CXCR4 inhibitor AMD3100 mobilizes T cells from the BM and the thymi in wild type mice (29). Consistent with our conclusions, it has been previously shown in wild type mice that CXCR4 overexpression or elevated CXCL12 levels in the BM lead to T cell accumulation, increased BM homing, and peripheral lymphopenia (36, 51–53).

In addition to oto-sino-pulmonary bacterial infections, WHIM patients have difficulty clearing infection with HPV and in some cases herpes simplex virus, and there are reports of HPV- and EBV-driven neoplasms in patients (5, 8, 54, 55). Other viral infections, including herpesvirus infections, do not clearly occur more frequently or with more severity in WHIM patients than in healthy individuals (8). In particular, in our cohort of 47 WHIM patients

that we have been studying for 17 years, we have a few patients with herpes simplex infections and patients with a history of chickenpox, but no patients with unusually severe or persistent herpesvirus infections. The mechanism for HPV susceptibility in the subset of WHIM patients with problematic warts is not defined and could include defects in antibody production or dendritic cell function, not only T lymphopenia. In this regard, we have previously reported the case of a unique patient WHIM patient WHIM-09 who was cured of WHIM syndrome by chromothriptic deletion of the WHIM allele solely in the myeloid cell lineage, which included complete regression of her warts in the face of persistence of the WHIM R334X genotype in all lymphoid cells (33). Our results show that WHIM $CD8^+$ T cells are competent in responding to acute LCMV infection in mice, which we used because the role of $CD8^+$ T cells, the focus of our paper, is particularly well-defined. To our knowledge, our LCMV challenge is the first acute viral challenge study conducted in WHIM mice. The normal LCMV-specific response is consistent with the clinical observations in patients and with our data showing that WHIM patient PBMCs have normal proliferative responses to mitogens, cytokines, vaccine antigens (Tetanus toxoid) and pathogen antigens (*Candida albicans*), consistent with the lack of persistent opportunistic infections in WHIM patients controlled by T cell immunity (with the exception of HPV) (unpublished data).

The BM is a preferred site for homeostatic proliferation of memory $CD8^+$ T cells. Neutrophils have been reported to be able to capture virus from the dermis, the site of antigen delivery, and to prime naïve $CD8^+$ T cells in the BM via resident myeloid antigen-presenting cells (56). In this regard, we speculate that neutrophil mobilization by AMD3100 may assist with antigen presentation and delivery to BM $CD8^+$ T cells, which are abundant in the WHIM BM, possibly facilitating virus clearance from the host. However, this is clearly insufficient for an effective anti-HPV response since WHIM patients have not shown clinically significant wart regression when treated with G-CSF, which selectively mobilizes neutrophils to the blood. Additional myeloid cell populations are also likely to be involved in the antiviral response, consistent with wart regression and 100% non-WHIM myeloid chimerism in WHIM-09 (33). In this patient, it is possible that myeloid cells that lost the WHIM mutation were able to capture HPV more efficiently and present HPV antigens to WHIM T cells in the BM to mount an effective immune response for virus clearance. Furthermore, CXCR4 on $CD4^+$ T cells has been reported to provide costimulatory signals during T cell activation, which may be altered in WHIM syndrome due to defective T cell:antigen-presenting cell conjugate formation (57–61). Therefore, it is possible that a combination of fewer circulatory T and antigen-presenting cells and a dampened adaptive response contributes to the establishment and persistence of HPV in WHIM patients (8, 62).

In conclusion, *Cxcr4* gain-of-function mutations in WHIM syndrome result in sequestration of mature CD8 SP thymocytes and T cells in the thymus and BM, respectively, contributing to peripheral T cell lymphopenia in WHIM mice. The mechanisms involve prolonged residence time in the thymus, enhanced homing to BM and accumulation in the BM. Future work will be necessary to understand the changes in TCR repertoire in WHIM patients and WHIM mice, and the compartmentalization of leukocytes including $CD8^+$ T cells in WHIM mice during ageing and after infection, both of which dynamically affect the thymus, BM and intraorgan CXCL12 levels (63–66).

Supplementary Material

Refer to Web version on PubMed Central for supplementary material.

Acknowledgments

We thank Dr. Alfred Singer for kindly providing us with RAG-GFP mice and Dr. Ulrich Siebenlist for the LCMV Armstrong strain. We also thank Dr. Shakuntala Rampertaap and Dr. Sergio D. Rosenzweig for providing the data for healthy donors. We thank Dr. Ainhoa Perez-Diez for assisting with *ex vivo* experiments and Melanie S. Vacchio with S1PR1 staining. Fig. 5B was created in BioRender.com.

This work was supported by the Division of Intramural Research, National Institute of Allergy and Infectious Diseases, National Institutes of Health.

Abbreviations used in this article:

BM	bone marrow
DN	double negative
DP	double positive
hi	high
iLNs	inguinal lymph nodes
lo	low
LCMV	lymphocytic choriomeningitis virus
mLN	mesenteric lymph node
MPECs	memory precursor effector cells
RTEs	recent thymic emigrants
SLECs	short-lived effector cells
SP	single positive
WHIM	warts, hypogammaglobulinemia, infections and myelokathexis

References

1. Ma Q, Jones D, Borghesani PR, Segal RA, Nagasawa T, Kishimoto T, Bronson RT, and Springer TA. 1998. Impaired B-lymphopoiesis, myelopoiesis, and derailed cerebellar neuron migration in CXCR4- and SDF-1-deficient mice. Proc. Natl. Acad. Sci. U.S.A 95: 9448–9453. [PubMed: 9689100]
2. Nagasawa T, Hirota S, Tachibana K, Takakura N, Nishikawa S, Kitamura Y, Yoshida N, Kikutani H, and Kishimoto T. 1996. Defects of B-cell lymphopoiesis and bone-marrow myelopoiesis in mice lacking the CXC chemokine PBSF/SDF-1. Nature 382: 635–638. [PubMed: 8757135]
3. Tachibana K, Hirota S, Iizasa H, Yoshida H, Kawabata K, Kataoka Y, Kitamura Y, Matsushima K, Yoshida N, Nishikawa S, Kishimoto T, and Nagasawa T. 1998. The chemokine receptor CXCR4 is essential for vascularization of the gastrointestinal tract. Nature 393: 591–594. [PubMed: 9634237]

4. Zou Y-R, Kottmann AH, Kuroda M, Taniuchi I, and Littman DR. 1998. Function of the chemokine receptor CXCR4 in haematopoiesis and in cerebellar development. Nature 393: 595–599. [PubMed: 9634238]
5. Balabanian K 2005. WHIM syndromes with different genetic anomalies are accounted for by impaired CXCR4 desensitization to CXCL12. Blood 105: 2449–2457. [PubMed: 15536153]
6. Hernandez PA, Gorlin RJ, Lukens JN, Taniuchi S, Bohinjec J, Francois F, Klotman ME, and Diaz GA. 2003. Mutations in the chemokine receptor gene CXCR4 are associated with WHIM syndrome, a combined immunodeficiency disease. Nat. Genet 34: 70–74. [PubMed: 12692554]
7. Eash KJ, Greenbaum AM, Gopalan PK, and Link DC. 2010. CXCR2 and CXCR4 antagonistically regulate neutrophil trafficking from murine bone marrow. J. Clin. Invest 120: 2423–2431. [PubMed: 20516641]
8. Heusinkveld LE, Majumdar S, Gao J-L, McDermott DH, and Murphy PM. 2019. WHIM Syndrome: from Pathogenesis Towards Personalized Medicine and Cure. J Clin Immunol 39: 532–556. [PubMed: 31313072]
9. Dotta L, Notarangelo LD, Moratto D, Kumar R, Porta F, Soresina A, Lougaris V, Plebani A, Smith CIE, Norlin A-C, Gòmez Raccio AC, Bubanska E, Bertolini P, Amendola G, Visentini M, Fiorilli M, Venuti A, and Badolato R. 2019. Long-Term Outcome of WHIM Syndrome in 18 Patients: High Risk of Lung Disease and HPV-Related Malignancies. The Journal of Allergy and Clinical Immunology: In Practice 7: 1568–1577. [PubMed: 30716504]
10. Majumdar S, and Murphy P. 2018. Adaptive Immunodeficiency in WHIM Syndrome. IJMS 20: 3. [PubMed: 30577453]
11. Evans MO, Petersen MM, Khojah A, Jyonouchi SC, Edwardson GS, Khan YW, Connelly JA, Morris D, Majumdar S, McDermott DH, Walter JE, and Murphy PM. 2021. TREC Screening for WHIM Syndrome. J Clin Immunol 41: 621–628. [PubMed: 33415666]
12. Gulino AV 2004. Altered leukocyte response to CXCL12 in patients with warts hypogammaglobulinemia, infections, myelokathexis (WHIM) syndrome. Blood 104: 444–452. [PubMed: 15026312]
13. Calderon L, and Boehm T. 2011. Three chemokine receptors cooperatively regulate homing of hematopoietic progenitors to the embryonic mouse thymus. Proceedings of the National Academy of Sciences 108: 7517–7522.
14. Plotkin J, Prockop SE, Lepique A, and Petrie HT. 2003. Critical role for CXCR4 signaling in progenitor localization and T cell differentiation in the postnatal thymus. J. Immunol 171: 4521–4527. [PubMed: 14568925]
15. Robertson P, Means TK, Luster AD, and Scadden DT. 2006. CXCR4 and CCR5 mediate homing of primitive bone marrow–derived hematopoietic cells to the postnatal thymus. Experimental Hematology 34: 308–319. [PubMed: 16543065]
16. Janas ML, Varano G, Gudmundsson K, Noda M, Nagasawa T, and Turner M. 2010. Thymic development beyond β-selection requires phosphatidylinositol 3-kinase activation by CXCR4. Journal of Experimental Medicine 207: 247–261. [PubMed: 20038597]
17. Trampont PC, Tosello-Trampont A-C, Shen Y, Duley AK, Sutherland AE, Bender TP, Littman DR, and Ravichandran KS. 2010. CXCR4 acts as a costimulator during thymic β-selection. Nature Immunology 11: 162–170. [PubMed: 20010845]
18. Lucas B, White AJ, Parnell SM, Henley PM, Jenkinson WE, and Anderson G. 2017. Progressive Changes in CXCR4 Expression That Define Thymocyte Positive Selection Are Dispensable For Both Innate and Conventional αβT-cell Development. Scientific Reports 7.
19. Balabanian K, Brotin E, Biajoux V, Bouchet-Delbos L, Lainey E, Fenneteau O, Bonnet D, Fiette L, Emilie D, and Bachelerie F. 2012. Proper desensitization of CXCR4 is required for lymphocyte development and peripheral compartmentalization in mice. Blood 119: 5722–5730. [PubMed: 22438253]
20. Gao J-L, Yim E, Siwicki M, Yang A, Liu Q, Azani A, Owusu-Ansah A, McDermott DH, and Murphy PM. 2018. Cxcr4-haploinsufficient bone marrow transplantation corrects leukopenia in an unconditioned WHIM syndrome model. Journal of Clinical Investigation 128: 3312–3318. [PubMed: 29715199]

21. Yu W, Nagaoka H, Jankovic M, Misulovin Z, Suh H, Rolink A, Melchers F, Meffre E, and Nussenzweig MC. 1999. Continued RAG expression in late stages of B cell development and no apparent re-induction after immunizion. Nature 400: 682–687. [PubMed: 10458165]
22. Kulinski JM, Eisch R, Young ML, Rampertaap S, Stoddard J, Monsale J, Romito K, Lyons JJ, Rosenzweig SD, Metcalfe DD, and Komarow HD. 2020. Skewed Lymphocyte Subpopulations and Associated Phenotypes in Patients with Mastocytosis. The Journal of Allergy and Clinical Immunology: In Practice 8: 292–301.e2. [PubMed: 31319217]
23. Majumdar S, Deobagkar-Lele M, Adiga V, Raghavan A, Wadhwa N, Ahmed SM, Rananaware SR, Chakraborty S, Joy O, and Nandi D. 2017. Differential susceptibility and maturation of thymocyte subsets during Salmonella Typhimurium infection: insights on the roles of glucocorticoids and Interferon-gamma. Sci Rep 7: 40793. [PubMed: 28091621]
24. Webb LV, Ley SC, and Seddon B. 2016. TNF activation of NF-κB is essential for development of single-positive thymocytes. Journal of Experimental Medicine 213: 1399–1407. [PubMed: 27432943]
25. Xu X, Zhang S, Li P, Lu J, Xuan Q, and Ge Q. 2013. Maturation and Emigration of Single-Positive Thymocytes. Clinical and Developmental Immunology 2013: 1–11.
26. Jaiswal H, Ciucci T, Wang H, Tang W, Claudio E, Murphy PM, Bosselut R, and Siebenlist U. 2021. The NF-κB regulator Bcl-3 restricts terminal differentiation and promotes memory cell formation of CD8+ T cells during viral infection. PLoS Pathog 17: e1009249. [PubMed: 33508001]
27. Kadakia T, Tai X, Kruhlak M, Wisniewski J, Hwang I-Y, Roy S, Guinter TI, Alag A, Kehrl JH, Zhuang Y, and Singer A. 2019. E-protein–regulated expression of CXCR4 adheres preselection thymocytes to the thymic cortex. Journal of Experimental Medicine 216: 1749–1761. [PubMed: 31201207]
28. Goedhart M, Gessel S, der Voort R, Slot E, Lucas B, Gielen E, Hoogenboezem M, Rademakers T, Geerman S, Buul JD, Huveneers S, Dolstra H, Anderson G, Voermans C, and Nolte MA. 2019. CXCR4, but not CXCR3, drives CD8 $^{+}$ T-cell entry into and migration through the murine bone marrow. Eur. J. Immunol 49: 576–589. [PubMed: 30707456]
29. Liu Q, Li Z, Gao J-L, Wan W, Ganesan S, McDermott DH, and Murphy PM. 2015. CXCR4 antagonist AMD3100 redistributes leukocytes from primary immune organs to secondary immune organs, lung, and blood in mice: Leukocyte signaling. European Journal of Immunology 45: 1855–1867. [PubMed: 25801950]
30. Freitas C, Wittner M, Nguyen J, Rondeau V, Biajoux V, Aknin M-L, Gaudin F, Beaussant-Cohen S, Bertrand Y, Bellanné-Chantelot C, Donadieu J, Bachelerie F, Espéli M, Dalloul A, Louache F, and Balabanian K. 2017. Lymphoid differentiation of hematopoietic stem cells requires efficient Cxcr4 desensitization. Journal of Experimental Medicine 214: 2023–2040. [PubMed: 28550161]
31. Boursalian TE, Golob J, Soper DM, Cooper CJ, and Fink PJ. 2004. Continued maturation of thymic emigrants in the periphery. Nat Immunol 5: 418–425. [PubMed: 14991052]
32. Hale JS, and Fink PJ. 2009. Back to the thymus: peripheral T cells come home. Immunol Cell Biol 87: 58–64. [PubMed: 19030016]
33. McDermott DH, Gao J-L, Liu Q, Siwicki M, Martens C, Jacobs P, Velez D, Yim E, Bryke CR, Hsu N, Dai Z, Marquesen MM, Stregevsky E, Kwatemaa N, Theobald N, Long Priel DA, Pittaluga S, Raffeld MA, Calvo KR, Maric I, Desmond R, Holmes KL, Kuhns DB, Balabanian K, Bachelerie F, Porcella SF, Malech HL, and Murphy PM. 2015. Chromothriptic Cure of WHIM Syndrome. Cell 160: 686–699. [PubMed: 25662009]
34. Lancaster JN, Li Y, and Ehrlich LIR. 2018. Chemokine-Mediated Choreography of Thymocyte Development and Selection. Trends in Immunology 39: 86–98. [PubMed: 29162323]
35. Butz EA, and Bevan MJ. 1998. Massive Expansion of Antigen-Specific CD8+ T Cells during an Acute Virus Infection. Immunity 8: 167–175. [PubMed: 9491998]
36. Khan AB, Carpenter B, Santos e Sousa P, Pospori C, Khorshed R, Griffin J, Velica P, Zech M, Ghorashian S, Forrest C, Thomas S, Gonzalez Anton S, Ahmadi M, Holler A, Flutter B, Ramirez-Ortiz Z, Means TK, Bennett CL, Stauss H, Morris E, Lo Celso C, and Chakraverty R. 2018. Redirection to the bone marrow improves T cell persistence and antitumor functions. Journal of Clinical Investigation 128: 2010–2024. [PubMed: 29485974]

37. De Clercq E 2019. Mozobil® (Plerixafor, AMD3100), 10 years after its approval by the US Food and Drug Administration. Antivir Chem Chemother 27: 204020661982938.
38. McDermott DH, Liu Q, Ulrick J, Kwatemaa N, Anaya-O'Brien S, Penzak SR, Filho JO, Priel DAL, Kelly C, Garofalo M, Littel P, Marquesen MM, Hilligoss D, DeCastro R, Fleisher TA, Kuhns DB, Malech HL, and Murphy PM. 2011. The CXCR4 antagonist plerixafor corrects panleukopenia in patients with WHIM syndrome. Blood 118: 4957–4962. [PubMed: 21890643]
39. McDermott DH, Liu Q, Velez D, Lopez L, Anaya-O'Brien S, Ulrick J, Kwatemaa N, Starling J, Fleisher TA, Priel DAL, Merideth MA, Giuntoli RL, Evbuomwan MO, Littel P, Marquesen MM, Hilligoss D, DeCastro R, Grimes GJ, Hwang ST, Pittaluga S, Calvo KR, Stratton P, Cowen EW, Kuhns DB, Malech HL, and Murphy PM. 2014. A phase 1 clinical trial of long-term, low-dose treatment of WHIM syndrome with the CXCR4 antagonist plerixafor. Blood 123: 2308–2316. [PubMed: 24523241]
40. McDermott DH, Pastrana DV, Calvo KR, Pittaluga S, Velez D, Cho E, Liu Q, Trout HH, Neves JF, Gardner PJ, Bianchi DA, Blair EA, Landon EM, Silva SL, Buck CB, and Murphy PM. 2019. Plerixafor for the Treatment of WHIM Syndrome. N Engl J Med 380: 163–170. [PubMed: 30625055]
41. Sugiyama T, Kohara H, Noda M, and Nagasawa T. 2006. Maintenance of the Hematopoietic Stem Cell Pool by Cxcl12-Cxcr4 Chemokine Signaling in Bone Marrow Stromal Cell Niches. Immunity 25: 977–988. [PubMed: 17174120]
42. Chaix J, Nish SA, Lin W-HW, Rothman NJ, Ding L, Wherry EJ, and Reiner SL. 2014. Cutting Edge: CXCR4 Is Critical for CD8 $^{+}$ Memory T Cell Homeostatic Self-Renewal but Not Rechallenge Self-Renewal. J.I 193: 1013–1016.
43. Mazo IB, Honczarenko M, Leung H, Cavanagh LL, Bonasio R, Weninger W, Engelke K, Xia L, McEver RP, Koni PA, Silberstein LE, and von Andrian UH. 2005. Bone Marrow Is a Major Reservoir and Site of Recruitment for Central Memory CD8+ T Cells. Immunity 22: 259–270. [PubMed: 15723813]
44. Schabath R, Müller G, Schubel A, Kremmer E, Lipp M, and Förster R. 1999. The murine chemokine receptor CXCR4 is tightly regulated during T cell development and activation. J Leukoc Biol 66: 996–1004. [PubMed: 10614783]
45. Halkias J, Melichar HJ, Taylor KT, Ross JO, Yen B, Cooper SB, Winoto A, and Robey EA. 2013. Opposing chemokine gradients control human thymocyte migration in situ. J. Clin. Invest 123: 2131–2142. [PubMed: 23585474]
46. Kim CH, Pelus LM, White JR, and Broxmeyer HE. 1998. Differential chemotactic behavior of developing T cells in response to thymic chemokines. Blood 91: 4434–4443. [PubMed: 9616136]
47. Poznansky MC, Olszak IT, Evans RH, Wang Z, Foxall RB, Olson DP, Weibrecht K, Luster AD, and Scadden DT. 2002. Thymocyte emigration is mediated by active movement away from stroma-derived factors. Journal of Clinical Investigation 109: 1101–1110. [PubMed: 11956248]
48. Vianello F, Kraft P, Mok YT, Hart WK, White N, and Poznansky MC. 2005. A CXCR4-dependent chemorepellent signal contributes to the emigration of mature single-positive CD4 cells from the fetal thymus. J. Immunol 175: 5115–5125. [PubMed: 16210615]
49. Zehentmeier S, Lim VY, Ma Y, Fossati J, Ito T, Jiang Y, Tumanov AV, Lee H-J, Dillinger L, Kim J, Csomos K, Walter JE, Choi J, and Pereira JP. 2022. Dysregulated stem cell niches and altered lymphocyte recirculation cause B and T cell lymphopenia in WHIM syndrome. Sci. Immunol 7: eabo3170.
50. Baran-Gale J, Morgan MD, Maio S, Dhalla F, Calvo-Asensio I, Deadman ME, Handel AE, Maynard A, Chen S, Green F, Sit RV, Neff NF, Darmanis S, Tan W, May AP, Marioni JC, Ponting CP, and Holländer GA. 2020. Ageing compromises mouse thymus function and remodels epithelial cell differentiation. eLife 9: e56221. [PubMed: 32840480]
51. Arieta Kuksin C, Gonzalez-Perez G, and Minter LM. 2015. CXCR4 expression on pathogenic T cells facilitates their bone marrow infiltration in a mouse model of aplastic anemia. Blood 125: 2087–2094. [PubMed: 25647836]
52. Leng Q, Nie Y, Zou Y, and Chen J. 2008. Elevated CXCL12 expression in the bone marrow of NOD mice is associated with altered T cell and stem cell trafficking and diabetes development. BMC Immunol 9: 51. [PubMed: 18793419]

53. Sawada S, Gowrishankar K, Kitamura R, Suzuki M, Suzuki G, Tahara S, and Koito A. 1998. Disturbed CD4+ T Cell Homeostasis and In Vitro HIV-1 Susceptibility in Transgenic Mice Expressing T Cell Line–tropic HIV-1 Receptors. Journal of Experimental Medicine 187: 1439–1449. [PubMed: 9565636]
54. Meuris F, Carthagena L, Jaracz-Ros A, Gaudin F, Cutolo P, Deback C, Xue Y, Thierry F, Doorbar J, and Bachelerie F. 2016. The CXCL12/CXCR4 Signaling Pathway: A New Susceptibility Factor in Human Papillomavirus Pathogenesis. PLoS Pathog 12: e1006039. [PubMed: 27918748]
55. Pastrana DV, Peretti A, Welch NL, Borgogna C, Olivero C, Badolato R, Notarangelo LD, Gariglio M, FitzGerald PC, McIntosh CE, Reeves J, Starrett GJ, Bliskovsky V, Velez D, Brownell I, Yarchoan R, Wyvill KM, Uldrick TS, Maldarelli F, Lisco A, Sereti I, Gonzalez CM, Androphy EJ, McBride AA, Van Doorslaer K, Garcia F, Dvoretzky I, Liu JS, Han J, Murphy PM, McDermott DH, and Buck CB. 2018. Metagenomic Discovery of 83 New Human Papillomavirus Types in Patients with Immunodeficiency. mSphere 3: e00645–18. [PubMed: 30541782]
56. Duffy D, Perrin H, Abadie V, Benhabiles N, Boissonnas A, Liard C, Descours B, Reboulleau D, Bonduelle O, Verrier B, Van Rooijen N, Combadière C, and Combadière B. 2012. Neutrophils Transport Antigen from the Dermis to the Bone Marrow, Initiating a Source of Memory CD8+ T Cells. Immunity 37: 917–929. [PubMed: 23142782]
57. Contento RL, Molon B, Boularan C, Pozzan T, Manes S, Marullo S, and Viola A. 2008. CXCR4-CCR5: a couple modulating T cell functions. Proc. Natl. Acad. Sci. U.S.A 105: 10101–10106. [PubMed: 18632580]
58. Kallikourdis M, Trovato AE, Anselmi F, Sarukhan A, Roselli G, Tassone L, Badolato R, and Viola A. 2013. The CXCR4 mutations in WHIM syndrome impair the stability of the T-cell immunologic synapse. Blood 122: 666–673. [PubMed: 23794067]
59. Kumar A, Humphreys TD, Kremer KN, Bramati PS, Bradfield L, Edgar CE, and Hedin KE. 2006. CXCR4 physically associates with the T cell receptor to signal in T cells. Immunity 25: 213–224. [PubMed: 16919488]
60. Nanki T, and Lipsky PE. 2000. Cutting edge: stromal cell-derived factor-1 is a costimulator for CD4+ T cell activation. J. Immunol 164: 5010–5014. [PubMed: 10799853]
61. Smith X, Schneider H, Köhler K, Liu H, Lu Y, and Rudd CE. 2013. The chemokine CXCL12 generates costimulatory signals in T cells to enhance phosphorylation and clustering of the adaptor protein SLP-76. Sci Signal 6: ra65.
62. Gallego C, Vétillard M, Calmette J, Roriz M, Marin-Esteban V, Evrard M, Aknin M-L, Pionnier N, Lefrançois M, Mercier-Nomé F, Bertrand Y, Suarez F, Donadieu J, Ng LG, Balabanian K, Bachelerie F, and Schlecht-Louf G. 2021. CXCR4 signaling controls dendritic cell location and activation at steady state and in inflammation. Blood 137: 2770–2784. [PubMed: 33512478]
63. Hernández-López C, Varas A, Sacedón R, Martínez VG, Hidalgo L, Valencia J, Zapata AG, and Vicente Á. 2010. The CXCL12/CXCR4 Pair in Aged Human Thymus. Neuroimmunomodulation 17: 217–220. [PubMed: 20134207]
64. Majumdar S, and Nandi D. 2018. Thymic Atrophy: Experimental Studies and Therapeutic Interventions. Scand. J. Immunol 87: 4–14. [PubMed: 28960415]
65. Periyasamy-Thandavan S, Burke J, Mendhe B, Kondrikova G, Kolhe R, Hunter M, Isales CM, Hamrick MW, Hill WD, and Fulzele S. 2019. MicroRNA-141–3p Negatively Modulates SDF-1 Expression in Age-Dependent Pathophysiology of Human and Murine Bone Marrow Stromal Cells. The Journals of Gerontology: Series A 74: 1368–1374.
66. Pritz T, Weinberger B, and Grubeck-Loebenstein B. 2014. The aging bone marrow and its impact on immune responses in old age. Immunology Letters 162: 310–315. [PubMed: 25014741]

Key points

- CXCR4 mutation in WHIM patients and mice elevates blood CD4/CD8 T cell ratios.
- WHIM CD8 T cells accumulate in the thymus and bone marrow of mice.
- T cell lymphopenia in WHIM mice is ameliorated by the CXCR4 antagonist, AMD3100.

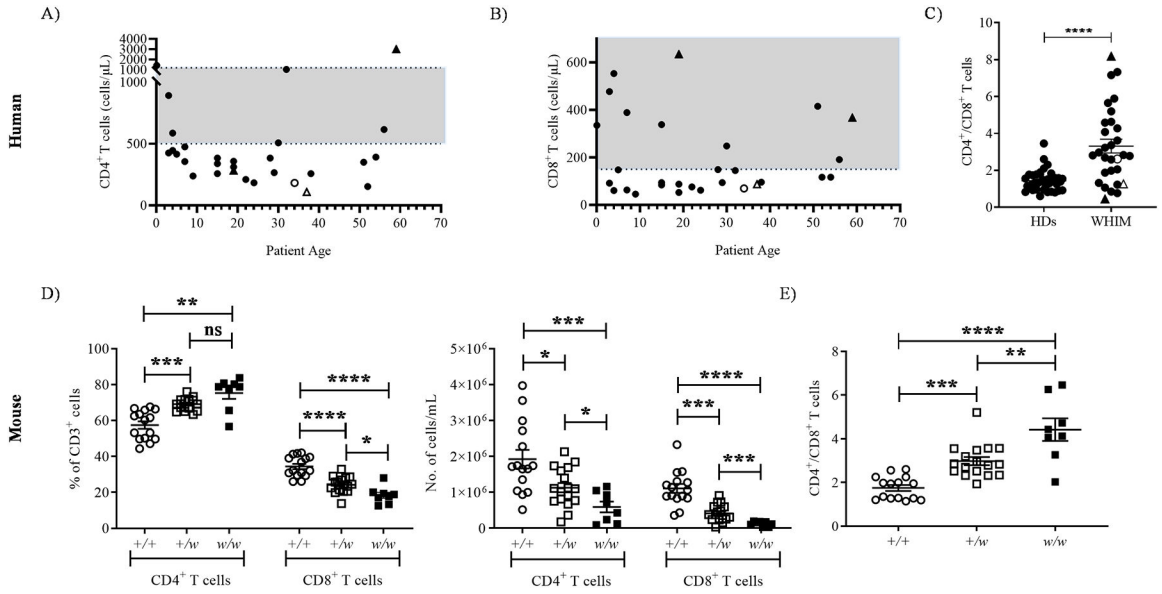

Figure 1: Severe CD8$^+$ T cell lymphopenia in WHIM patients and WHIM model mice.

Circulating T lymphocytes were analyzed at the first visit of WHIM patients to the NIH, when they were not receiving cell-mobilizing agents and showed no signs of active infection. **A and B)** T cell lymphopenia in NIH WHIM patients. Absolute numbers of the indicated T cell subsets were plotted as a function of patient age at presentation to the NIH. **C)** CD4/CD8 ratios in WHIM patients. The ratios were calculated from the source data in panels **A** and **B**. The WHIM patients included 18 females and 12 males, with a median age of 23.8 years (ranging from neonates to 59 years). Healthy donor (HD) data in **C** were derived from 21 female and 16 male NIH blood donors, with a median age of 46 years (ranging from 22–68 years). Upright triangle symbols designate patients who had had splenectomy and unfilled symbols designate patients carrying the CXCR4 S338X mutation. The shaded gray areas in the graphs **A** and **B** are normal ranges for adults at the NIH Clinical Center Department of Laboratory Medicine. **D)** T cell lymphopenia in 5–8 week old WHIM mice. CD4$^+$ and CD8$^+$ T cell subset frequency in the CD3$^+$ gate (left panel) and total counts (right panel) in the blood. **E)** CD4/CD8 ratios in blood calculated from the data in panel **D**. In **D** and **E**, mouse *Cxcr4* genotypes (*+*, wild type allele; *w*, WHIM knockin allele) are shown on the x-axes, and each dot corresponds to data from one mouse from at least 8 mice per genotype from 8 independent experiments. Data in panels **C**-**E** are the mean ± SEM. ns, not significant; *, p< 0.05, **, p< 0.01, ***, p< 0.001 and ****, p< 0.0001 as determined by the two-tailed unpaired t test for **C** and one-way ANOVA for **D** and **E**.

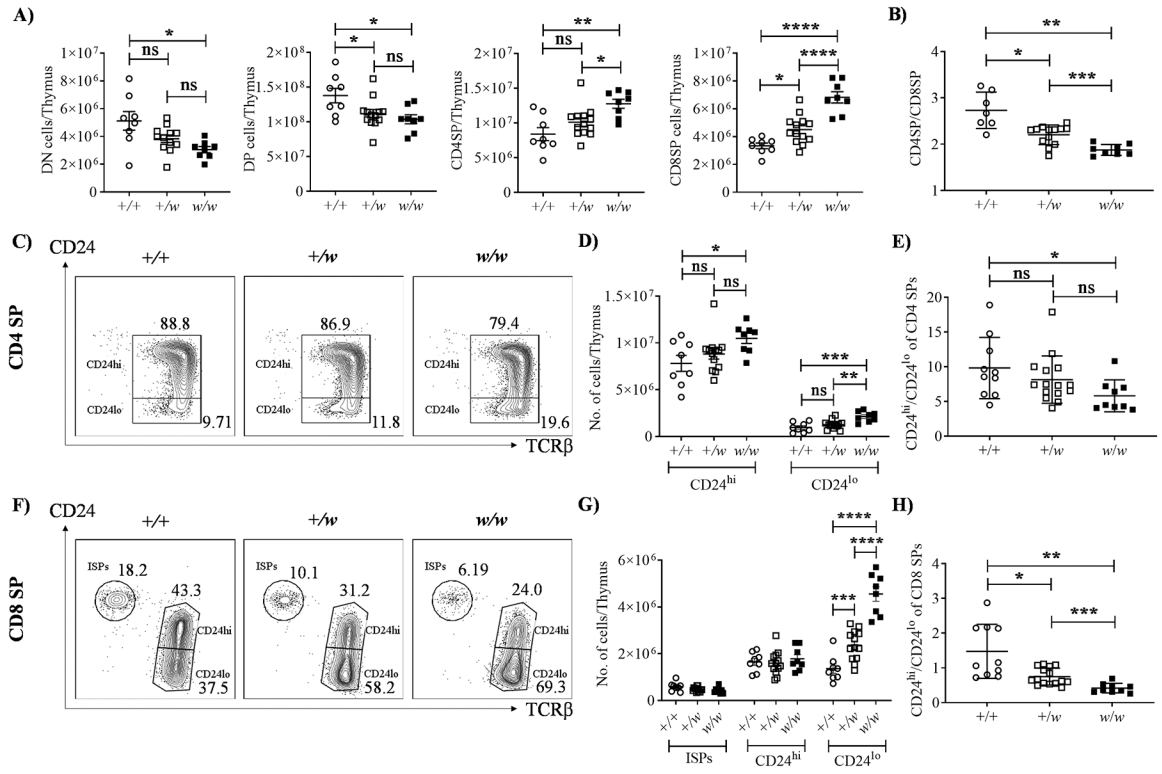

Figure 2: Accumulation of CD8 SP thymocytes in WHIM mice results from selective increase of mature CD24^{lo}CD8 SP cells.

5–8 week old mice were sacrificed, thymi were harvested, and thymocytes were analyzed by flow cytometry. **A)** Thymocyte subset analysis by CD4 and CD8 expression. Summary data are shown for the absolute numbers of thymocyte subsets. **B)** CD4/CD8 ratios. **C-H)** SP subset analysis by CD24 and TCRβ expression. **C-E)** Analysis of CD4 SP. **F-H)** Analysis of CD8 SP. **C and F)** Representative contour-plots for CD4 and CD8 SP cells, respectively. *Cxcr4* genotypes (+, wild type allele; *w*, WHIM allele) are indicated at the top of each plot. ISP, immature CD8 single positive cells (CD24^{hi}TCRβ^{lo}). The subset names and frequencies are adjacent to each gate. In **D** and **G**, the immature single positives (ISPs, CD24^{hi}TCRβ^{lo}), CD24^{hi}TCRβ^{hi} (semi-mature) and CD24^{lo}TCRβ^{hi} (mature) cells were gated and their absolute counts per thymus are summarized for all mice tested. The ratios of CD24^{hi}/CD24^{lo} cells in the CD4 SP and CD8 SP compartments were also calculated **(E and H)**. The *Cxcr4* genotypes of the mouse groups in **A, B, D, E, G** and **H** are indicated on the x-axes. Each dot corresponds to data from one mouse. Data are summarized as the mean ± SEM of at least 7 mice per genotype from 4 independent experiments. ns, not significant; *, p< 0.05, **, p< 0.01, ***, p< 0.001 and ****, p< 0.0001 as determined by the one-way ANOVA for all the data sets.

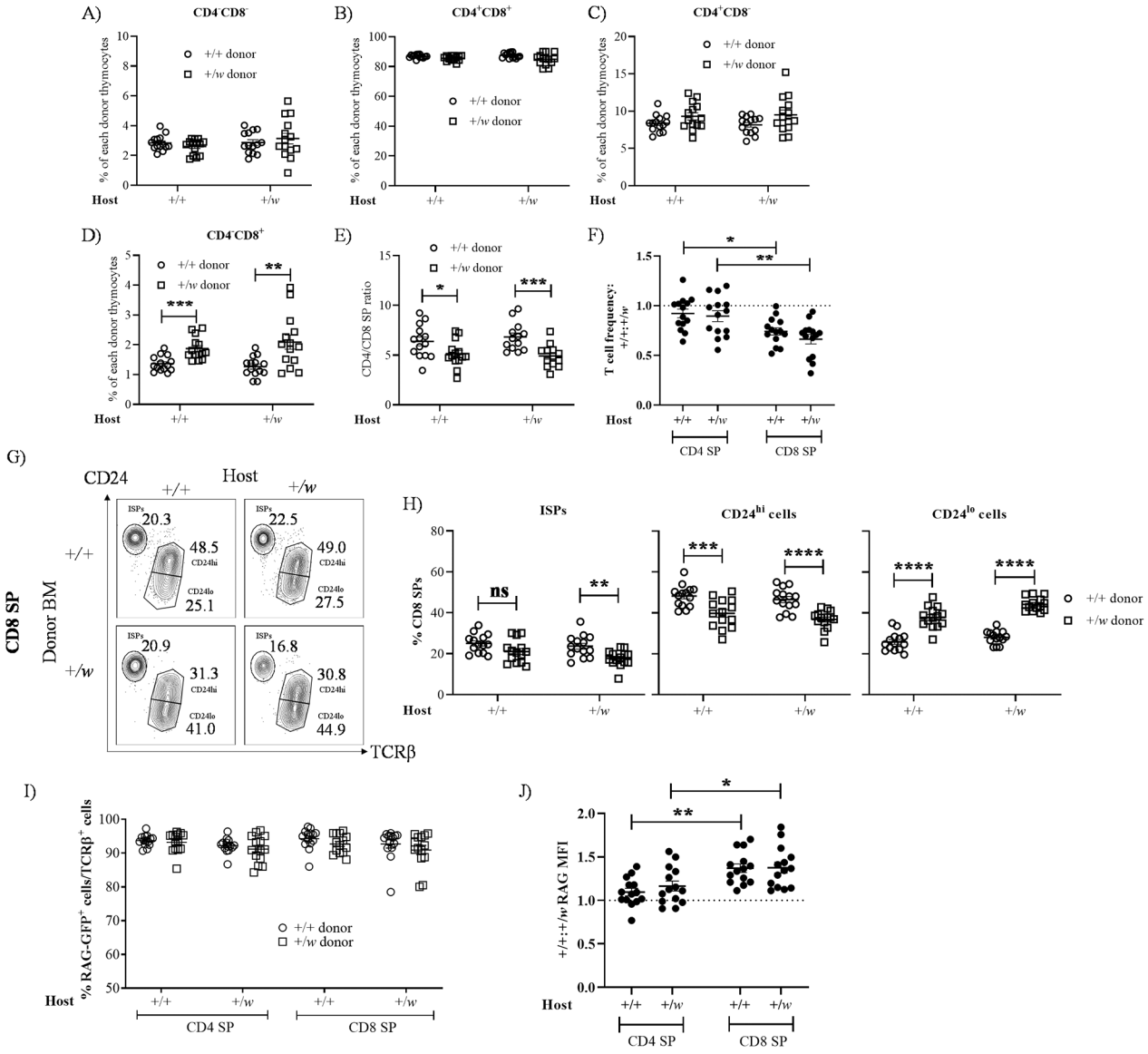

Figure 3: Accumulation of WHIM CD8 SP thymocytes in the thymus is cell-intrinsic and associated with prolonged thymic residence.

Approximately 6-week-old male and female CD45.1/.2 +/+ and CD45.2 +/*w* mice transgenic for RAG-GFP were sacrificed, and their BM cells were harvested. After T cell depletion, the +/+ and +/*w* BM cells were mixed at a 1:1 ratio and injected i.v. into lethally irradiated CD45.1/.2 +/+ and CD45.1/.2 +/*w* recipient mice (not expressing RAG-GFP). 8–10 weeks after transplantation, thymi were harvested and the proportions of major thymocyte subsets were quantified by FACS analysis for the subsets indicated above each graph in **A-D**. **E)** CD4/CD8 SP ratios. Ratios were calculated from data in panels **C** and **D**. In **A-E**, the *Cxcr4* genotypes for the donor-derived thymocytes and host groups are indicated in the insets and on the x-axes, respectively. **F)** +/+/ to +/*w* SP ratios for the SP cells and host groups indicated on the x-axis. **G and H)** The WHIM mutation promotes accumulation of mature CD24^{lo}CD8 SP donor cells in the thymus. **G)** Representative contour-plots for the CD24 and TCRβ staining of CD8 SP cells. The recipient and donor *Cxcr4* genotypes

(+, wild type Cxcr4; *w*, WHIM allele) are designated for each graph column and row, respectively; ISP, immature single positive cells ($CD24^{hi}TCR\beta^{lo}$). The subset names and frequencies are adjacent to each gate. **H)** Summary data for ISPs, $CD24^{hi}$ and $CD24^{lo}$ CD8 SP subsets, respectively. The *Cxcr4* genotypes of the donor cells are given in the legend on the right. **I and J)** Prolonged thymic residence time of mature +/*w* $CD24^{lo}$CD8 SPs. The proportions of RAG-GFP-positive CD4 and CD8 SP $TCR\beta^{+}$ thymocytes were quantified in **I**. The *Cxcr4* genotypes of the donor cells are given in the inset. **J)** Donor +/+ to +/*w* ratios of the geometric mean fluorescence intensity (MFI) of RAG-GFP expression for the SP subsets and hosts indicated on the x-axis. Data are summarized as the mean ± SEM of 16 mice per genotype from 7 independent experiments. *, $p< 0.05$, ****, $p< 0.01$, ***, $p< 0.001$ and ****, $p< 0.0001$, as determined by multiple t-tests for panels **D**, **E** and **H**, and the one-way ANOVA for panels **F** and **J**.

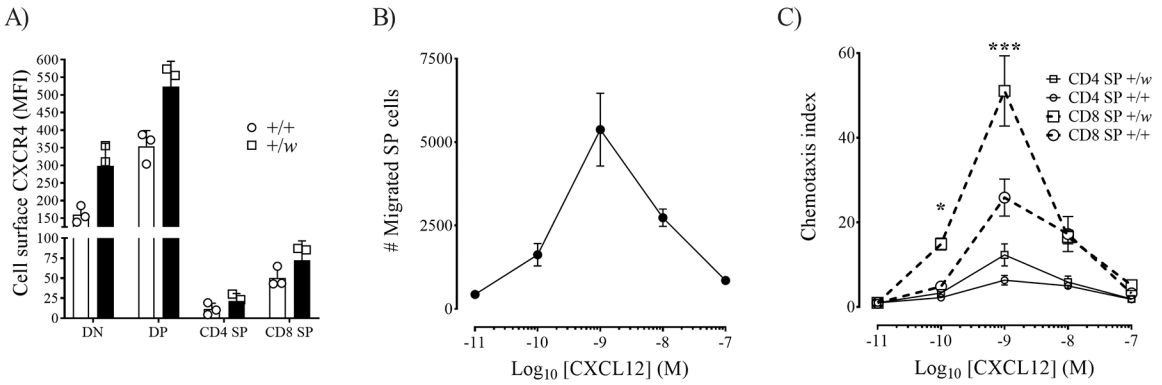

Figure 4: Enhanced CXCL12-mediated chemotactic responses by CD8 SP thymocytes from WHIM model mice.

6–8 weeks-old male and female +/+ and +/*w* mice were sacrificed, and their thymi were harvested. **A)** Cell-surface CXCR4 expression on TCRβ$^+$ SP thymocytes from the mouse genotypes indicated in the inset (+, wild type *Cxcr4*; *w*, WHIM allele). Bars represent mean ± SD CXCR4 median fluorescence intensity (MFI) of 3 mice (white symbols) analyzed in duplicate. Data are from one experiment representative of 4 independent experiments and analyzed by multiple t-test. **B and C)** CXCL12-induced chemotaxis of SP thymocytes. After processing the thymi of +/+ and +/*w* mice, CD4 and CD8 SP thymocytes were isolated by magnetic-activated cell sorting, and then were differentially stained with green and violet calcein AM before pooling the 4 SP populations together. Chemotactic responses of this SP pool to increasing doses of mouse CXCL12 (x-axes) were tested in transwell assays and migrated cells were counted and analyzed by FACS. **B)** Total number of migrating SP cells. **C)** Chemotaxis index for each SP subset. The *Cxcr4* genotype (+, wild type; *w*, WHIM allele) code for **A** and **C** is indicated in the inset. In **B** and **C**, data are the mean ± SEM of 3 independent experiments analyzed in quadruplicates. *, p<0.05; ***, p< 0.001, as determined by two-way ANOVA for the CD8 SP +/w vs CD8 SP +/+ comparison.

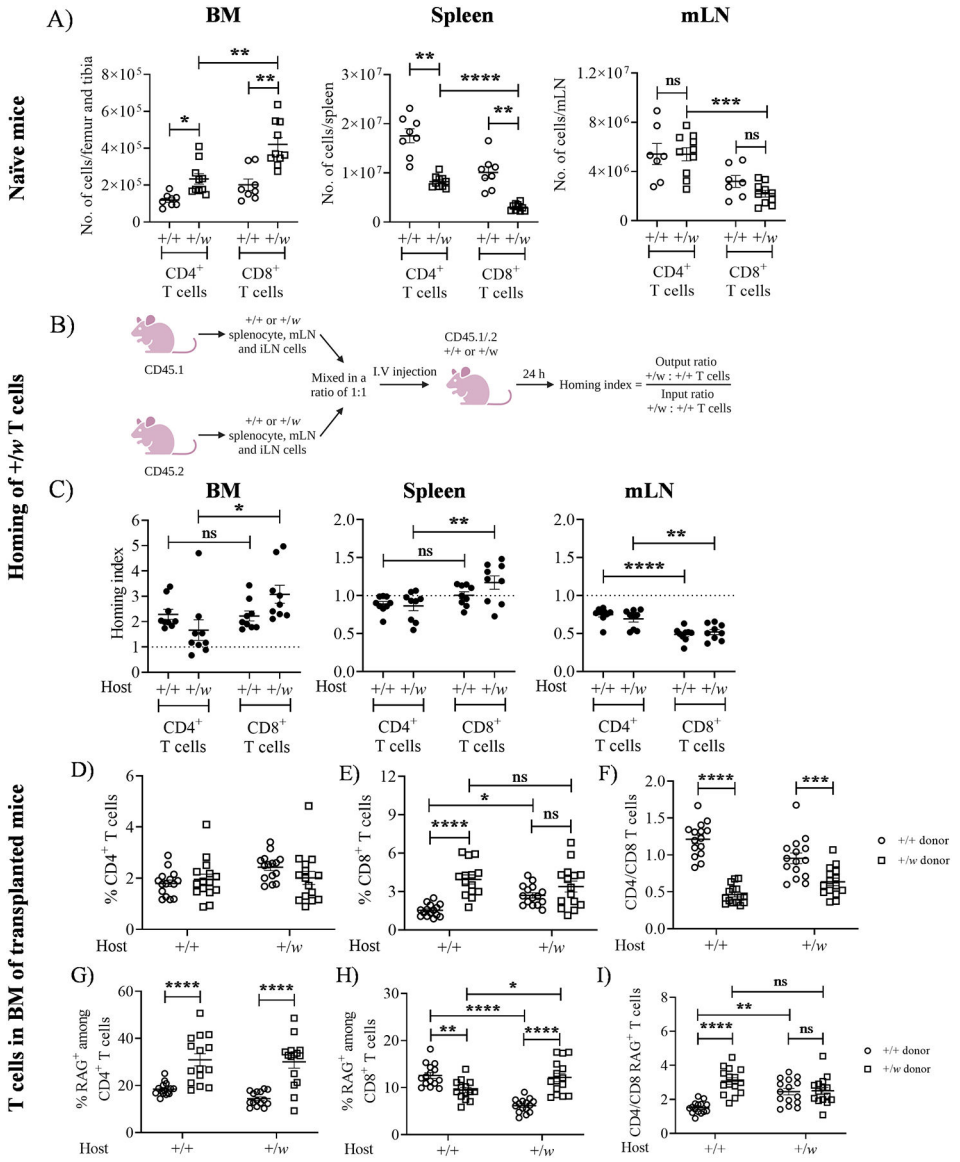

Figure 5: WHIM CXCR4 enhances T cell residence in the BM.

A) Higher T cell content in the BM of +/*w* mice. 5–8 weeks-old +/+ and +/*w* mice were sacrificed, their BM, spleen and mesenteric lymph node (mLN) were harvested and the organs were processed to quantify the T cell content. For panel **A**, data from 4 independent experiments consisting of at least 8 mice/genotype are summarized. The *Cxcr4* genotypes of the mice are given on the x-axes of the graphs. **(B and C)** +/*w* CXCR4 enhances T cell entry into the BM. **B)** Experimental protocol for quantification of T cell homing index. CD45 isoform-marked cells from spleen, mLN and iLN of 8–12 weeks-old +/+ and +/*w* mice were harvested and processed. The +/+ and +/*w* cells were mixed in a ratio of 1:1 and injected i.v. into CD45.1/.2 +/+ and +/*w* mice. After 24 h of adoptive transfer, organs in the host mice were harvested to quantify the donor T cell content. **(C)** Homing capacity of +/*w* T cells. The samples indicated on the top of each panel were harvested and stained to quantify the T cell content. The *Cxcr4* genotypes of the recipient mice are given on the x-axis of

each panel. Data are summarized as the mean ± SEM of 8–9 mice per genotype from 3 independent experiments. **(D-I)** +/*w* $CD8^+$ T cells accumulate in the BM in a cell-intrinsic manner. T-cell depleted CD45.1/.2 +/+ and CD45.2 +/*w* BM expressing RAG-GFP were mixed in a ratio of 1:1 and injected i.v. into lethally irradiated CD45.1/.2 +/+ and +/*w* recipient mice (not expressing RAG-GFP). After 8–10 weeks of BM reconstitution, the femurs and tibias were harvested and T cells in the BM were studied. Total donor $CD4^+$ **(D)** and $CD8^+$ **(E)** T cells were quantified as percentages of total $CD45^+$ cells, which were then used to calculate donor-specific CD4/CD8 ratios **(F)**. The RAG-GFP^+ cells among donor $CD4^+$ T cells (**G)** and donor $CD8^+$ T cells (**H)** were also quantified as a percentage of $CD4^+$ and $CD8^+$ cells, respectively, which were then used to calculate the corresponding CD4/CD8 ratios (**I)**. The *Cxcr4* genotypes of the recipient mice are indicated on the x-axes. The *Cxcr4* genotypes of the donor-derived T cells are given in the legends on the right side of panels **F** and **I**. Data are summarized as the mean ± SEM of 16 mice per genotype from 7 independent experiments. ns: not significant, *, $p< 0.05$, **, $p< 0.01$ and *** $p< 0.001$, ****, $p< 0.0001$ as determined by the one-way ANOVA for **A** and **C** and two-way ANOVA for **D-I**.

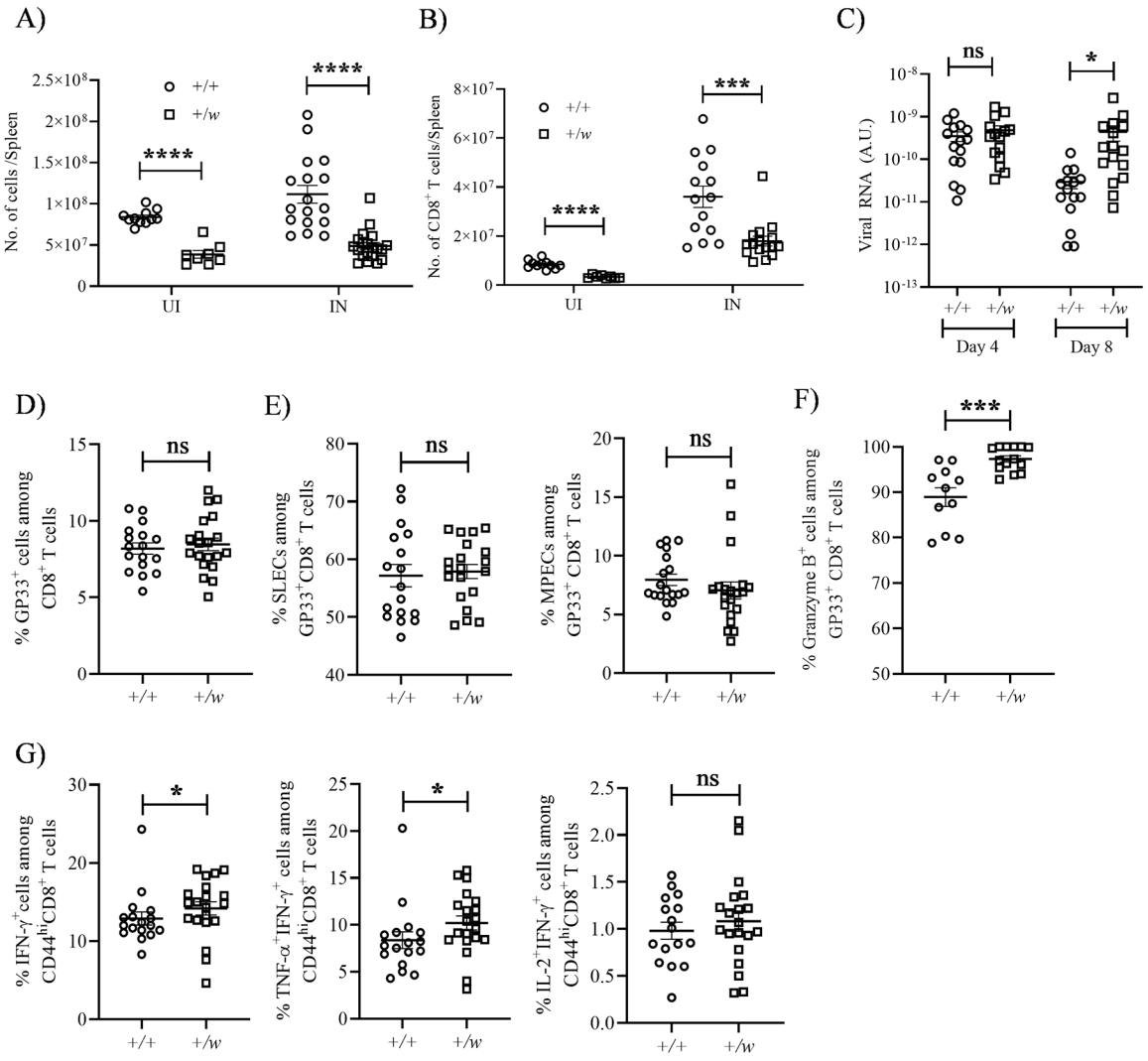

Figure 6: WHIM CD8$^+$ T cells undergo normal activation and differentiation in response to acute LCMV infection.

+/+ and +/*w* mice were infected i.p. with 2 × 10^5 plaque forming units/mouse of LCMV (Armstrong strain). On day 8 after infection, infected and uninfected mice were sacrificed, and their splenocytes were analyzed by FACS. **(A and B)** Total splenic cellularity and CD8$^+$ T cell numbers. The *Cxcr4* genotypes and infection status are indicated on the x-axes. +, wild type; *w*, WHIM; UI, uninfected; IN, infected. **(C)** Viral burden. The viral burdens in sera on days 4 and 8 post infection were quantified by RT-PCR for the conditions indicated on the x-axis. **(D and E)** Differentiation. **(D)** LCMV peptide GP33 tetramer-specific CD8$^+$ T cells were gated to quantify the **(E)** SLEC (short lived effector cells, KLRG1^{hi}CD127/IL-7Rα^{lo}) and MPEC (memory precursor effector cells, KLRG1^{lo}CD127/IL-7Rα^{hi}) subsets. **(F and G)** Activation. The proportions of LCMV-specific CD8$^+$ T cells expressing the factors shown at the top of each panel were quantitated by intracellular staining. **(G)** Cytokines were measured after *in vitro* stimulation of GP33$^+$CD44$^+$ splenocytes. The *Cxcr4* genotypes of the mouse groups are shown as insets in **A** and **B** and on the x-axes for **C**-**G**. +, wild type; *w*, WHIM allele. Data are summarized as the mean ± SEM of at least 8 mice

per genotype from 3–4 independent experiments. ns: not significant, *, p< 0.05, ***, p< 0.001 and ****, p< 0.0001 as determined by the two-tailed unpaired t test for **A-D**, **E** (left panel), **F** and **G** (right most panel) and Mann Whitney test for **E** (right panel) and **G** (first two panels).

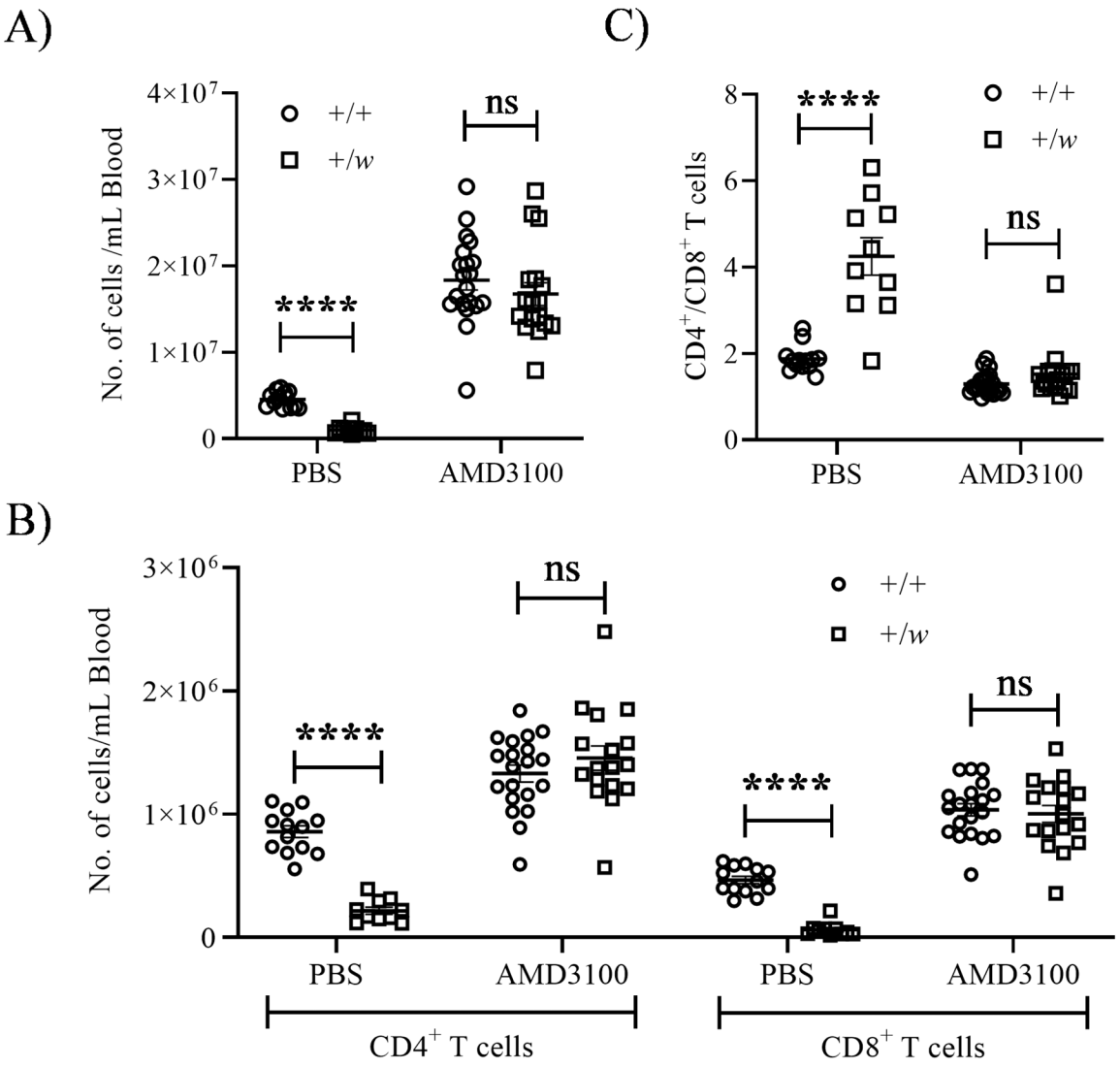

Figure 7: Inhibition of CXCR4 with the antagonist AMD3100 corrects T cell lymphopenia and normalizes the CD4/CD8 ratio in the blood of WHIM mice.

Naïve +/+ and +/*w* mice were administered either PBS or 10 mg/kg of AMD3100 via the i.p. route. 2.5 h after injection, blood samples were collected and analyzed. **(A)** Total leukocyte count. **(B)** Absolute $CD4^+$ and $CD8^+$ T cell counts. **(C)** CD4/CD8 ratios. The *Cxcr4* genotype (+, wild type; *w*, WHIM allele) code for all panels is shown as insets of the graphs. Data are summarized as the mean ± SEM of at least 10 mice per genotype from 10 independent experiments. ns: not significant, ****, $p < 0.0001$ as determined by the multiple t-test.

Table 1:

Effects of the WHIM CXCR4^{1013} (p.S338X) mutation on the absolute T cell numbers in naïve +/+ mice compared to +/*w* littermates (× 10^6 cells ± SEM) and on the abundance of +/*w* cells relative to +/+ cells in reconstituted +/+ and +/*w* hosts. Significant differences between +/+ (not underlined) and +/*w* (underlined) are marked in bold.

	Cell populations	Naïve mice (# × 10^6 in +/+ mice vs. +/*w* mice)	Transplanted mice	
			+/+ hosts (% donor cells)	+/*w* hosts (% donor cells)
Blood	CD4$^+$ T cells	**1.92±0.2vs.1.13±0.1**	20.54±1.2vs.28.64±3.0	18.04±1.9vs.22.88±3.3
	CD8$^+$ T cells	**1.1±0.1vs.0.41**	8.78±0.6vs.6.8±0.6	7.14±0.7vs.5.38±0.7
	CD4/CD8	**1.74±0.1vs.2.97±0.2**	**2.45±0.2vs.4.23±0.3**	**2.56±0.1vs.4.38±0.4**
Thymus	CD4 SP	8.39±0.9vs.11.01±0.6	8.37±0.3vs.9.3±0.5	8.16±0.3vs.9.51±0.6
	CD8 SP	**3.33±0.2vs.4.5±0.3**	**1.33±0.7vs.1.87±0.1**	**1.26±0.1vs.2.08±0.2**
	CD4/CD8 SP	**2.73±0.1vs.2.18±0.1**	**6.38±0.4vs.5.13±0.3**	**6.83±0.4vs.4.91±0.3**
	CD24^{hi}CD4SP	7.81±0.8vs.8.82±0.5	88.93±0.4vs.87.55±0.7	87.15±0.6vs.84±0.8
	CD24^{lo}CD4SP	0.96±0.2vs.1.27±0.1	9.37±0.5vs.10.9±0.6	11.01±0.7vs.14.13±0.9
	CD24^{hi}CD8SP	1.65±0.1vs.1.36±0.2	**48.21±1.4vs.39.75±1.9**	**46.5±1.5vs.36.75±1.2**
	CD24^{lo}CD8SP	**1.59±0.1vs.2.36±0.2**	**25.86±1.2vs.37.77±1.4**	**28.06±0.8vs.44.25±0.9**
Spleen	CD4$^+$ T cells	**17.55±1.4vs.8.21±0.4**	28.23±0.9vs.27.07±1.5	28.1±0.8vs.24.36±1.4
	CD8$^+$ T cells	**10.09±1.2vs.3.01±0.2**	9.22±0.3vs.9.16±0.5	**8.62±0.2vs.6.82±0.3**
	CD4/CD8	**1.79±0.1vs.2.78±0.1**	3.09±0.1vs.3.03±0.2	3.28±0.1vs.3.57±0.1
BM	CD4$^+$ T cells	**0.11vs.0.233**	1.79±0.1vs.1.95±0.2	2.42±0.1vs.2.01±0.2
	CD8$^+$ T cells	**0.2vs.0.42**	**1.52±0.1vs.3.93±0.3**	2.69±0.2vs.3.38±0.4
	CD4/CD8	0.62vs.0.55	**1.21vs.0.46**	**0.95±0.1vs.0.63**
mLN	CD4$^+$ T cells	5.41±0.8vs.5.40±0.5	**42.10±1.0vs.31.16±1.5**	**43.82±0.9vs.35.23±1.2**
	CD8$^+$ T cells	3.12±0.5vs.2.19±0.3	**18.51±0.5vs.11.4±0.8**	**16.66±0.3vs.10.55±0.4**
	CD4/CD8	**1.69vs.2.53±0.1**	**2.29±0.1vs.2.84±0.2**	**2.64±0.1vs.3.38±0.1**
iLN	CD4$^+$ T cells	1.59vs.1.29±0.1	45.48±1.8vs.50.09±2.4	44.94±1.5vs.50.32±2.0
	CD8$^+$ T cells	**0.93±0.1vs.0.44**	**20.18±0.9vs.15.61±0.9**	**20.74±0.7vs.14.74±0.6**
	CD4/CD8	**1.69±0.1vs.2.98±0.1**	**2.3±0.1vs.3.35±0.2**	**2.18±0.1vs.3.47±0.2**